INFORMATICA, 2006, Vol. 17, No. 2, 225–236

A Multiresolution Approach Based on MRF and Bak–Sneppen Models for Image Segmentation

Kamal E. MELKEMI
University of Biskra, Computer Science Department, 07000 Biskra, Algeria and
University of Constantine, Vision Group, LIRE laboratory, 25000 Constantine, Algeria
e-mail: melkemi@mailcity.com

Mohamed BATOUCHE,
University of Constantine, Vision Group, LIRE laboratory, 25000 Constantine, Algeria
e-mail: batouche@wissal.dz

Sebti FOUFOU
University of Burgundy, LE2I laboratory, UFR sciences, BP 47870, 21078 Dijon Cedex, France
e-mail: sfoufou@u-bourgogne.fr

Received: October 2004

Abstract. The two major Markov Random Fields (MRF) based algorithms for image segmentation are the Simulated Annealing (SA) and Iterated Conditional Modes (ICM). In practice, compared to the SA, the ICM provides reasonable segmentation and shows robust behavior in most of the cases. However, the ICM strongly depends on the initialization phase.

In this paper, we combine Bak–Sneppen model and Markov Random Fields to define a new image segmentation approach. We introduce a multiresolution technique in order to speed up the segmentation process and to improve the restoration process. Image pixels are viewed as lattice species of Bak–Sneppen model. The a-posteriori probability corresponds to a local fitness. At each cycle, some objectionable species are chosen for a random change in their fitness values. Furthermore, the change in the fitness of each species engenders fitness changes for its neighboring species. After a certain number of iteration, the system converges to a Maximum A Posteriori estimate. In this multireolution approach, we use a wavelet transform to reduce the size of the system.

Key words: image segmentation, Markov random fields, multiresolution, Bak–Sneppen, self-organized criticality.

1. Introduction

Image segmentation process partitions the image in a set of disjoint regions (Haralick and Shapiro, 1985) the union of which must correspond to the whole image. In this work, we are interested in a segmentation based on Markov Random Field (MRF) model (Geman and Geman, 1984; Besag, 1986; Derin and Elliott, 1987; Dubes *et al.*, 1990; Kato *et al.*, 1992). The problem considered is the estimation of a configuration of labels x from a set of pixels y. We cite the two main algorithms: The Simulated Annealing (SA) (Geman and Geman, 1984; Kirkpatrick *et al.*, 1983; Van Laarhoven and Aarts, 1987; Metropolis *et al.*, 1953) and the Besag's Iterated Conditional Modes (ICM) (Besag, 1986). Other segmentation methods based on Genetic Algorithms (GA) have also been proposed (Andrey and Tarroux, 1998; Kim *et al.*, 2000). The SA approach (Geman and Geman, 1984; Kirkpatrick *et al.*, 1983; Van Laarhoven and Aarts, 1987; Metropolis *et al.*, 1953) is based on the combination of the Gibbs sampling and cooling schedule. It is inspired by simulation equilibrium behavior of large lattice-based systems.

In SA, controlling temperature is a very important task. The case of the schedule annealing is often quite difficult and the system can freezes into a local minimum. Theoretically, SA will always converge to global optimum. Unfortunately, SA remains a computationally intensive image segmentation method. The ICM is proposed as an alternative method to MAP estimation by J. Besag (Besag, 1986). Beginning by a sub-optimal configuration, the ICM maximizes the probability of the classification field by deterministically and iteratively changing pixel segmentations. The ICM algorithm (Dubes *et al.*, 1990) is computationally efficient. However, it strongly depends on the initialization phase and it converges to a local optima.

In this work, we present a new multiresolution based approach for image segmentation. First, we combine Bak–Sneppen model and Markov Random Fields to define a new image segmentation approach, and then we introduce a multiresolution technique to speed up the segmentation process and help the restoration process.

We present a Bak–Sneppen and MRFs combined approach for image segmentation called MRF-EO. In this MRF-EO approach, gray levels in image pixels are viewed as species in a lattice of Bak–Sneppen model (Bak *et al.*, 1987; Bak and Sneppen, 1993). Indeed, we use Extremal Optimization (EO) heuristic (Boettcher, 1999; Boettcher and Percus, 2001; Boettcher and Percus, 2003) motivated by the Bak–Sneppen mechanism. The Graph Bipartitioning is one popular hard optimization problem, to which EO has been applied successfully (Boettcher and Percus, 2000). Meshoul and Batouche (Meshoul and Batouche, 2002) use the EO algorithm on a standard cost function for aligning natural images.

At each cycle of evolution, some worst species are chosen for a random change in their fitness values. Moreover, the change in fitness value of each species engenders changes in the fitness value of its neighboring species. After a number of iterations, the species reorganize themselves in a set of categories, where each category represents an image region. The MRF-EO algorithm operates in two principal phases: The initialization phase consists in creating an *initial configuration* x. The update phase is the modification of the *current configuration* by: first, calculating the local fitness values for the current site labels. Second, choosing at random against some objectionable site labels. The novelty of our approach can be summarized in:

- the evolution aspect of the system is not imposed from outside;
- it updates only a single copy of the solution by selecting against the worst site labels;
- it is a non-equilibrium approach;
- it needs only minor parameters;

- it has an emergent capabilities.

As a consequence for its advantages, MRF-EO has to pay an overhead computational cost for evaluating and sorting the site labels. We have introduced a multiresolution technique in order speed-up the process and to improve the restoration aspect of the approach. We refer the resulting algorithm as MMRF-EO. The main idea of this approach is to reduce the size of the system using the FWT. Several approaches based on the reduction of the system size are proposed (Bouman and Shapiro, 1994; Liu and Yang, 1994).

The MMRF-EO based algorithm for image segmentation operates in three phases:

- First, we decompose the input discrete data corresponding to the observed image.
- Second, we perform the MRF-EO based algorithm on the approximation of input discrete data.
- Third, we reconstruct a successively higher resolution segmented images.

This paper is organized in four sections: the first section presents related concepts. The second section describes our algorithms. The third section is consecrated to preliminary results. The conclusion is given in the fourth section.

2. Related Concepts

2.1. *Definitions and Notations*

An image $S = \{1, .., t, .., MN\}$ specifies the gray levels for all pixels in an MN-lattice $(MN = M \times N)$, where t is called a site. The true and the observed images are represented by the random variable vectors $X = (X_1, .., X_t, .., X_{MN}),\ X_t \in \{1, .., C\}$ and $Y = (Y_1, .., Y_{MN}),\ Y_t \in \{0, .., 255\}$. Let Ω be the set of all possible configurations. We suppose that Y is the result of adding Gaussian noise process to the true image (Dubes *et al.*, 1990; Lakshmanan and Derin, 1989). A neighborhood system $N = (N_i \subset S,\ i \in S)$ is a subset collection N_i of S that verifies: (1) $i \notin N_i$ and (2) $j \in N_i \Leftrightarrow i \in N_j$. A clique c is a set of points which are all neighbors to each other: $\forall r,\ t \in c,\ r \in N_t$.

Let $X = (X_1, .., X_{MN}) \in \Omega$. We abbreviate $X = x$ the event $(X_1 = x_1, ..., X_{MN} = x_{MN})$. X is a MRF with respect to N if:

1. For all $x \in \Omega : P(X = x) > 0$.
2. For every $t \in S \quad x \in \Omega$: $P(x_i/x_j, j \in S - \{i\}) = P(x_i/x_j, j \in N_i)$.

X is a MRF on S with respect to N if and only if $P(X = x)$ is a Gibbs distribution defined by: $P(X = x) = e^{-U(x)}/Z$ where $Z = \sum_{x \in \Omega} e^{-U(x)}$ is the partition function and $U(x)$ is the energy function defined by:

$$U(x) = \sum_{t=1}^{MN} \sum_{r \in N_t} \theta_r \delta(x_t, x_r), \tag{1}$$

where θ_r are the clique parameters, $\delta(a, b) = -1$ if $a = b$, 1 if $a \neq b$. $P(X = x)$ is called the a-priori probability.

The a-posteriori probability $P(x/y)$ follows a Gibbs distribution given by: $P(x/y) = e^{-U(x/y)}/Z_y$ where Z_y is the normalization constant and $U(x/y)$ is the energy function (Kato *et al.*, 1992) given in Eq. 2:

$$U(x/y) = \sum_{t=1}^{MN} \left[\ln(\sqrt{2\Pi}\sigma_{xt}) + \frac{(y_t - \mu_{xt})^2}{2\sigma_{xt}^2} + \sum_{r \in N_t} (\beta\delta(x_t, x_r)) \right], \tag{2}$$

where β is a positive model parameter that controls the homogeneity of the image regions. We can define image segmentation as the estimation of configuration x which minimizes the fitness function $U(x/y)$. We call this approach the MAP estimation.

2.2. *Bak–Sneppen Model and EO Heuristic*

The Bak–Sneppen model of evolution (Bak and Sneppen, 1993) is a successful application of the Self-Organized Criticality (SOC) (Bak, 1996) concept. In this model, species are placed on lattice-system sites. Each species has a fitness value in $[0, 1]$, where the higher the fitness, the better the chance of species survival (Bak and Sneppen, 1993). Bak–Sneppen mechanism is expressed as a meta-heuristic called EO by Boettcher *et al.* (Boettcher, 1999; Boettcher and Percus, 2000; Boettcher and Percus, 2003) into two versions: the basic EO and the τ-EO version. In the τ-EO heuristic, the process is based on the selection against several objectionable variables. Indeed, all variables are selected for state-updating indiscriminately. This general modification yields the stochastic aspect of the meta-heuristic.

2.3. *The Fast Wavelet Transform Algorithm*

The Fast Wavelet Transform (FWT) is a wavelet representation which only requires a number of operations proportional to the size of the initial discrete data.

This algorithm links the orthonormal wavelet bases to classical tools of digital signal processing such as sub-band coding schemes and discrete filters.

The two dimension (2D) of this algorithm is not presented here (see (Mallat, 1998) and (Chui, 1992)), however one dimension FWT is briefly presented. The decomposition of a discrete signal (Y_k), is performed by applying a pair of low-pass and high-pass discrete filters (h_k) and (g_k) known as conjugate quadrature filters. This is followed by a decimation of two filters to keep the same total information:

$$Y_k^{(1)} = \sum_n h_{n-2k} Y_n^{(0)} \quad \text{and} \quad D_k^{(1)} = \sum_n g_{n-2k} Y_n^{(0)}. \tag{3}$$

It is then possible to iterate this decomposition process on the coarser approximation.

$$Y_k^{(0)} = \sum_n (h_{k-2n} Y_n^{(0)} + g_{k-2n} D_n^{(0)}). \tag{4}$$

3. The Proposed Image Segmentation Algorithms

We present two new algorithms for image segmentation.

3.1. *MRF-EO Based Algorithm*

We consider site labels as species and the image as lattice-system as in Bak–Sneppen model. The fitness value of species x_i is λ_i given by Eq. 5:

$$\lambda_i = P(x_i/x_j, j \in N_i). \tag{5}$$

We present the MRF-EO based algorithm as follows:

1) Input data $y^{(0)}$: $y^{(0)}$ represents the observed image of size $M \times N$.
2) Create an initial solution $x(0)$ (segmented image sized MN): The MRF-EO creates an initial sub-optimal configuration from the observed image using a K-means procedure.
   For $t = \{1, .., MN\}$ Do compute λ_t. Compute $U = U(x/y)$.
3) Let $x_{best} = x$, $F_{best} =$ and Iteration $= 1$.
4) Find a permutation π of site labels $x_t : \lambda_{\pi(1)} \leqslant \ldots \leqslant \lambda_{\pi(MN)}$.
   Example. In the Table 1, we suppose that $N_1 = 2$ and $M_1 = 3$. The site label x_2 is the worst site label and x_5 is the best site label.
5) For $s = 1..MN$ Do
   - Compute probability $P_s \propto s^{-\tau}$ where τ is a parameter (Boettcher, 2003).
   - Generate an uniform random number μ_s in $[0, 1]$.
   - If $\mu_s \leqslant P_s$ Then modify the label of the site $\pi(s)$.

   Example. In the Table 1, the MRF-EO based algorithm replaces the labels of the sites $\pi(1)$, $\pi(2)$ and $\pi(4)$.
6) For $t = 1..MN$ Do evaluate λ_t of x. Compute $U = U(x/y)$.
7) If $U > F_{best}$ Then $x_{best} = x$ and $F_{best} = U$.
8) Iteration = Iteration $+1$.
9) If (Iteration $\leqslant$ a given number of iterations) Then goto 4.
10) Output x_{best} and F_{best}.

Table 1
The selection and modification of the labels of the sites $\pi(1)$, $\pi(2)$ and $\pi(4)$

Site i	$i = 1$	$i = 2$	$i = 3$	$i = 4$	$i = 5$	$i = 6$
Site label x_i	x_1	x_2	x_3	x_4	x_5	x_6
Fitness value λ_i	0.53	0.1	0.35	0.63	0.8	0.25
$\pi(i)$	2	6	3	1	4	5
P_i	0.5	0.27	0.13	0.05	0.03	0.02
$\mu(i)$	0.38	0.25	0.15	0.025	0.5	0.8

We notice that the evolution of the system is not imposed from outside. In GA approaches used in image segmentation based on MRF (Andrey and Tarroux, 1998), crossovers operators perform global exchanges on a pair of configurations. In contrast, our algorithm uses only a single copy of the system, which is refined simply by updating some bad site labels. It is based on Bak–Sneppen mechanism, which yields an extremal dynamic optimization process free of selection parameters. The MRF-EO based algorithm is presented as a minimization process of $U(x/y)$ of $M \times N$ variables. Because of such $(M \times N)$ large number of variables the time used for this optimization is very long. In the next subsection, we improve this algorithm by the introduction of a multiresolution analysis step, which reduces the number of system variables to optimize. The resulting new algorithm called MMRF-EO decomposes the input data of size $M \times N$ in an approximation data of size $M/2^k \times N/2^k$ and errors called details. Then, it performs MRF-EO based algorithm on the approximation data and constructs the segmented image at the original resolution.

3.2. *Description of the Multiresolution MRF-EO Based Algorithm*

3.2.1. *The Wavelet-Decomposition*

This first phase is presented as follows:

1) input data $y^{(0)}$: $y^{(0)}$ is the observed image;
2) output data $y^{(k)}$: $y^{(k)}$ is the approximation of input discrete data at k-th lower resolution of size of $M_1 = (M/2^k) \times N_1 = (N/2^k)$.

3.2.2. *MRF-EO Segmentation of the Approximation of Input Discrete Data*

In this second phase, we perform MRF-EO based algorithm on the approximation input image $y^{(k)}$ as follows :

1) input data $y^{(k)}$: $y^{(k)}$ of size $M_1 \times N_1, M_1 = M/2^k$, $N_1 = N/2^k$;
2) output data $x^{(k)}$: $x^{(k)}$ of size $M_1 \times N_1$.

3.2.3. *Reconstruction of the Segmented Image at the Original Resolution*

In this third phase, we reconstruct a successively segmented images $x^{(k-1)} \dots x^{(0)}$. We repeat the following three steps until ($M_1 = M$ and $N_1 = N$). First, we transpose the segmented result $x^{(k)}$ of k-th lower resolution sized $M_1 \times N_1$ at a higher resolution $x^{(k-1)}$ using a quadtree structure. We represent the site $i = j + (M_1 - 1).l$ in $2D$ by the (j, l); we associate four site labels $x_{i1}, x_{i2}, x_{i3}, x_{i4}$ where $x_{i1} = x_{i2} = x_{i3} = x_{i4}$, and the sites $i1, i2, i3$ and $i4$ correspond to $(2j-1, 2l-1), (2j-1, 2l), (2j, 2l-1)$ and $(2j, 2l)$ respectively (see Fig. 1 (a)).

Second, we smooth errors detected near edges of the reconstructed segmented image (see Fig. 1 (b)). Let i be an edge site and (e, d) its $2D$ representation, then for each site (e, d) we:

1. Associate the four sites in segmented image $x^{(k+1)}$ at higher resolution: $(2 \times e - 1, 2 \times d - 1)$, $(2 \times e - 1, 2 \times d)$, $(2 \times e, 2 \times d - 1)$ and $(2 \times e, 2 \times d)$. We consider the neighbor sets of the four reconstructed sites of (e, d) (see Fig. 1(b)):

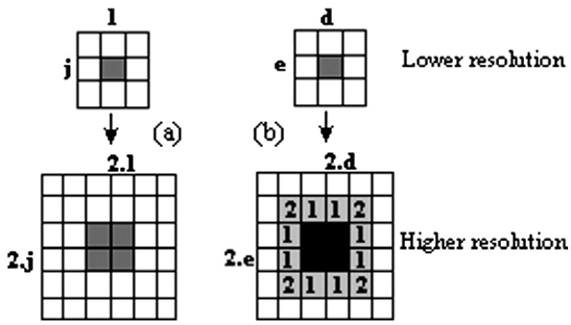

Fig. 1. (a) Site label reconstruction, (b) Edge reconstruction.

$N_{(2\times e-1,2\times d-1)} = \{(2\times e-1, 2\times d-2), (2\times e-2, 2\times d-2), (2\times e-2, 2\times d-1)\}$.
$N_{(2e-1,2d)} = \{(2 \times e-1, 2\times d+1), (2\times e-2, 2\times d), (2\times e-2, 2\times d+1)\}$.
$N_{(2\times e,2\times d-1)} = \{(2\times e, 2\times d-2), (2\times e+1, 2\times d-2), (2\times e+1, 2\times d-1)\}$.
$N_{(2e,2d)} = \{(2\times e, 2\times d+1), (2\times e+1, 2d), (2\times e+1, 2\times d+1)\}$.

2. Assign classes to the four site labels as follows (see Fig. 1(b)):
$x^{(k+1)}(2\times e-1, 2\times d-1)$ = arg min $\sqrt{(x(j,l)-m)^2}$ for $(j,l) \in N_{(2\times e-1,2\times d-1)}$ and m is the mean given by the following formula:
$m = \sum_{(j,l)\in N_{(2\times e-1,2\times d-1)}} x(j,l)/3$, etc...

Third, $M_1 = 2\times M_1$ and $N_1 = 2\times N_1$.

4. Experimental Results

We present one result of the MRF-EO compared with the ICM. We assume an isotropic second-order Ising model, so in equation 1, $\theta_1 = \theta_2 = \theta_3 = \theta_4 = \beta$. We have used one value of $\beta = 1.5$ which is kept constant through each segmentation. The segmentation is evaluated by both visual examination and energy function. The observed image y is the same starting discrete data for all algorithms given with the maximum likelihood estimate of the segmentation. In Fig. 2, we segment noisy scene containing a pyramid and a cube on a table. It can be seen that the different regions are well segmented using MRF-EO based algorithm despite the interference and the thinness of some regions whereas the ICM algorithm fails to do so.

In the experiment presented in Fig. 3, the observed image is corrupted by noise and the MRF-EO extracts the segments of the image better than the ICM.

In Fig. 4, we show the segmentation of a two gray-tones containing four geometric formes (rectangle, triangle, circle, star). It can be seen that despite the interference and the thinness of some regions the image is better segmented using MMRF-EO than MRF-EO algorithm. The justification of this result is due to decomposition phase which reduces noise in the observed image (see Fig. 4).

We deduce that the MRF-EO produces better segmentation results than the ICM. The major inconvenience of ICM resides in the fact that its convergence depends on the ini-

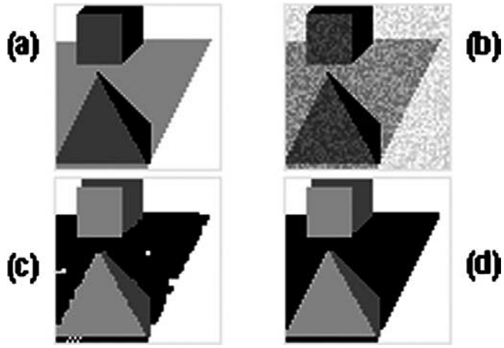

Fig. 2. (a) true image (b) noisy image, (c) ICM segmentation, (d) MRF-EO segmentation. Parameters: $\beta = 1.5, \tau = 1.3, C = 4$.

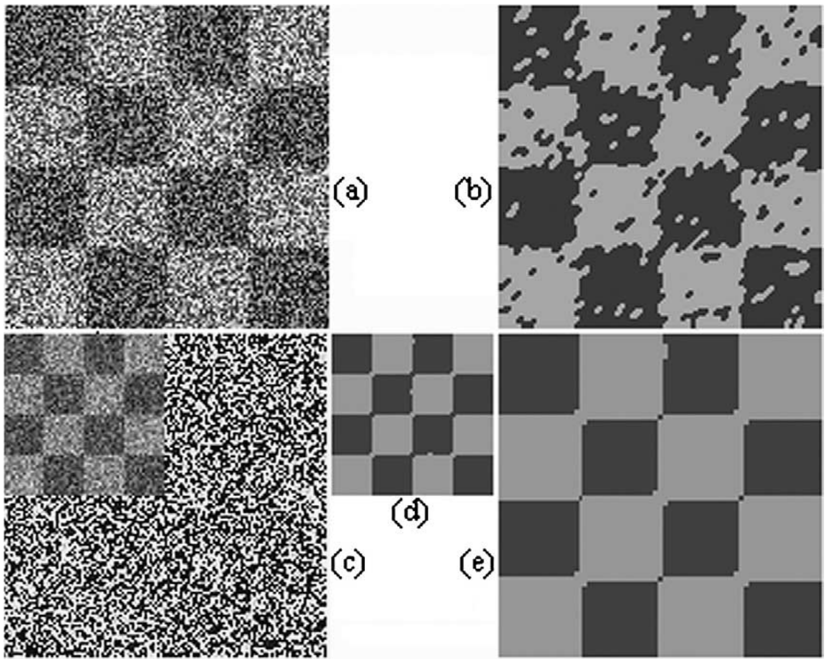

Fig. 3. Chess image segmentation. (a) noisy image 128×128, (b) MRF-EO segmented image, (c) FWT decomposition, (d) Segmentation at lower resolution (the second phase of MMRF-EO), (e) MMRF-EO segmented image. The parameters are $C = 2$, $\beta = 1.5$, τ=1.3, $k = 1$.

tial data. Segmentations on different images show that the MMRF-EO based algorithm performs better and requires much less computations than the MRF-EO algorithm for MAP estimation. The MMRF-EO algorithm combines the wavelet decomposition and the MRF-EO procedure in order to speed up the segmentation process. In Fig. 3, the segmentation using the MMRF-EO algorithm is reasonable and largely faster than the MRF-EO algorithm. These experiments were performed on a Pentium P4, CPU 2.66

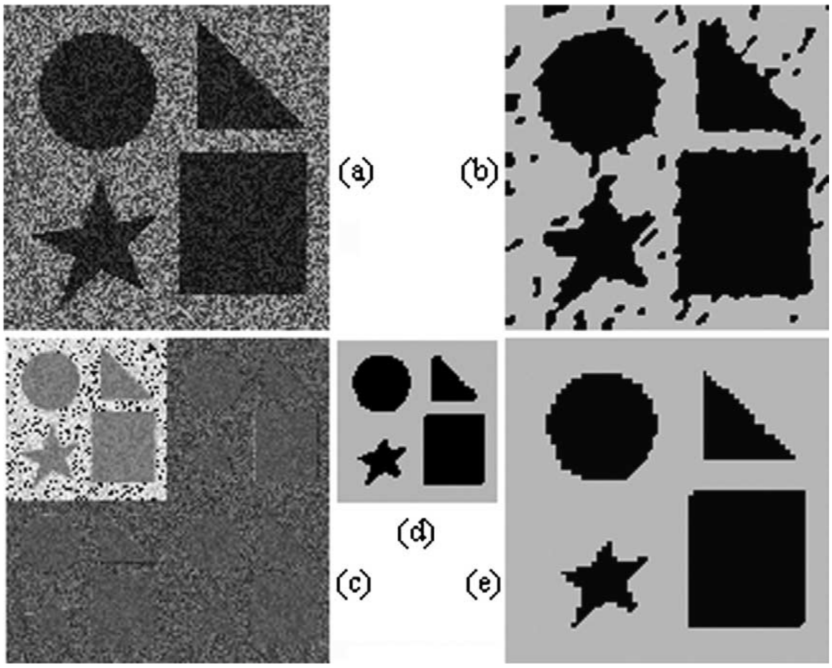

Fig. 4. A geometric figures at 128×128 resolution with two regions, $\beta = 1, 5$, $k = 1$).

GHz with 128 Mo of RAM. We performed the segmentation of chess figure (Fig. 3) at 512×512 resolution in 8 minutes and 45 seconds using the MRF-EO algorithm and in 4 minutes and 11 seconds using the MMRF-EO algorithm with the parameter value $k = 2$.

5. Conclusion

We have introduced a new MRF model-based approach for image segmentation. It is based on the Bak–Sneppen model. Indeed, site labels evaluated by the a-posteriori probabilities and their image represent the elements of the Bak–Sneppen model whose SOC's states are exactly the MAP estimates. Unlike the SA, the MRF-EO algorithm proceeds without need of any control parameter and optimal states of the system emerge naturally without any external intervention. The robustness of our approach is due to large fluctuations called avalanches which are result of the modification of several worst site labels. This co-evolutionary activity allows the process to explore new solutions in configuration space. We presented a multiresolution application which reduces the size of the system and allows a faster convergence of the process. Moreover, the advantage of the FWT decomposition reduces the noise in observed images which improves the segmentation results.

References

Andrey, P., and P. Tarroux (1998). Unsupervised segmentation of Markov random field modeled textured image using selectionist relaxation. *IEEE Trans. on PAMI*, **20**(3), 252–262.

Bak, P. (1996). *How Nature Works: The Scince Of Self-Organizd Criticality*. Springer, New York.

Bak, P., and K. Sneppen (1993). Punctuated equilibrium and criticality in a simple model of evolution. *Physical Rev. Letters*, **71**(24), 4083–4086.

Bak, P., C. Tang and K. Wiesenfeld (1987). Self-organized criticality: an explanation of the 1/f noise. *Physical Rev. Letters*, **59**(4), 381–384.

Besag, J. (1986). On the statistical analysis of dirty images. *Journal of Royal Statistics Society*, **48**, 259–302.

Boettcher, S. (1999). Extremal optimization and graph partitioning at the percolation threshold. *J. Physics A: Mathematical and General*, **32**(28), 5201–5211.

Boettcher, S. (2003). Extremal optimization. In Alexander K. Hartmann and Heiko Rieger (Eds.), *New Optimization Algorithms to Physics*. Wiley-VCH Verlag Berlin GmbH, Vol. 32(28), pp. 1–27.

Boettcher, S., and A.G. Percus (2000). Nature's way of optimizing. *Artificial Intelligence*, **119**(1–2), 275–286.

Boettcher, S., and A.G. Percus (2001). Extremal optimization for graph partitioning. *Phys. Rev. E.*, **64**(026114), 1–13.

Boettcher, S., and A.G. Percus (2001). Optimization with extremal dynamics. *Physical Rev. Letters*, **86**(23), 689–700.

Boettcher, S., and A.G. Percus (2003). Extremal optimization: an evolutionary local-search algorithm. In H.K. Bhargava and N. Ye (Eds.), series *Computational Modeling and Problem Solving in the Networked World*. Kluwer Academic Publishers.

Bouman, C.A., and M. Shapiro (1994). A multiscale random field model for Bayesian image segmentation. *IEEE Trans. on Image Processing*, **3**(2), 162–177.

Chui, C.K. (1998). *Wavelets: A Tutorial in Theory and Applications*. Academic Press.

Derin, H., and H. Elliott (1987). Modeling and segmentation of noisy and textured images using Gibbs random fields. *IEEE Trans. on PAMI*, **9**, 39–55.

Dubes, R.C., A.K. Jain, S.G. Nadabar and C.C. Chen (1990). MRF model-based algorithms for image segmentation. *IEEE Trans. on PAMI*, 808–814.

Geman, S., and D. Geman (1984). Stochastic relaxation, gibbs distributions, and the Bayesian restoration of images, *IEEE Trans. on PAMI*, **6**(6), 721–741.

Haralick, R.M., and L.G. Shapiro (1985). Survey: image segmentation. *Computer Vision, Graphics and Image Processing*, **29**, 100–132.

Kato, Z, T. Zerubia and M. Berthod (1992). Satellite image classification using a Metropolis dynamics. In *Proce. of ICQSSP*. San Francisco. pp. 808–814.

Kim, E.K, S.H. Park and H.J. Kim (2000). A genetic algorithm-based segmentation of Markov random field modeled images. *IEEE Signal Processing Letters*, **7**(11).

Kirkpatrick, S., C.D. Gelatt and M.P. Vecchi (1953). Optimization by simulated annealing. *Science*, **220**(4), 671–680.

Lakshmanan, S., and H. Derin (1989). Simultaneous parameter estimation ane segmentation of gibbs random fields using simulated annealing. *IEEE Trans. on PAMI*, **11**, 799–813.

Liu, J., and Y.H. Yang (1994). Multiresolution color image segmentation. *IEEE on PAMI*, **16**, 689–700.

Mallat, S.G. (1998). *A Wavelet Tour of Signal Processing*. Academic Press.

Meshoul, S., and M. Batouche (2002). Robust point correspondence for image registration using optimization with extremal dynamics. *Lect. Notes Comput. Sc.*, **2449**, 330–337.

Metropolis, N., A. Rosenbluth, M. Rosenbluth, A. Teller and E. Teller (1953). Equation of state calculation by fast computing machines. *Journal of Chem. Physics*, **21**, 1087–1092.

Van Laarhoven, P.J.M., and E.H.L. Aarts (1987). *Simulated Annealing: Theory and Applications*. Kluwer Academic Publishers. Edition D. Riedel.

K.E. Melkemi received his MSc and PhD degrees in computer science from the University of Batna, Algeria in 1993, and from the University of Constantine, Algeria, in 2006 respectively. Currently, he is a full associate professor at the Computer Science Department, University of Biskra, Algeria. His research areas include artificial life and pattern recognition.

M. Batouche received his MSc and PhD degrees in computer science from the Institut National Polytechnique de Lorraine (INPL), France, in 1989 and 1993, respectively. Currently, he is a full professor at the University of Constantine, Algeria. His research areas include artificial intelligence and pattern recognition.

S. Foufou obtained a PhD in computer science in 1997 from the University of Claude Bernard Lyon I, France, for a dissertation on parametric surfaces intersections. Since then, he is working as an associate professor in the Computer Science Department at the University of Burgundy, France. His research interests concern geometric modelling and CAD-CAM topics and include: surfaces blending using Dupin cyclides, subdivision surfaces, geometric constraints solving. Currently, he is working, as a guest researcher with the MSID-DPG group, at the National Institute of Standards and Technology, Gaithersburg, MD, USA, where he is contributing in product engineering related researches: product data representation, smart machining systems, tolerances, assembly modelling and PLM.

MRF ir Bak–Sneppen modeliais pagrįstas vaizdų segmentavimas

Kamal E. MELKEMI, Mohamed BATOUCHE, Sebti FOUFOU

Šiame straipsnyje pasiūlytas naujas vaizdų segmentavimo būdas, apjungiantis Bak–Sneppen modelį ir Markovo atsitiktinius laukus. Segmentavimo proceso pagreitinimui ir atstatymo proceso pagerinimui supažindinama su daugiarezoliuciniu metodu. Vaizdo taškai laikomi Bak–Sneppen modelio grotelių elementais. Aposteriorinė tikimybė atitinka lokalų tinkamumą. Kiekvieno ciklo metu dalies netinkamų elementų tinkamumo reikšmės pakeičiamos atsitiktinėmis. Be to tinkamumo pasikeitimas sukelia gretimų elementų tinkamumo pasikeitimą. Po tam tikro iteracijų skaičiaus sistema konverguoja į maksimalų aposteriorinį įvertį. Šiame metode sistemos sumažinimui naudojama bangelių transformacija.